A Three-Dimensional 64-Site Folded Electrode Array Using Planar Fabrication

Sister Mary Elizabeth Merriam, Onnop Srivannavit, Mayurachat Ning Gulari, and Kensall D. Wise, *Life Fellow, IEEE*

***Abstract*—Neuroscience and neuroprosthetic devices are increasingly in need of more compact less invasive 3-D electrode arrays for interfacing with neural tissue. To meet these needs, a folding 64-site 3-D array architecture has been developed. The microstructure, in which four probes and two platforms are fabricated as a single planar unit, results in a low-profile (< 350-μm) narrow-platform (0.604-mm^2 silicon footprint) implant for cortical use. Signals are routed from 177-μm^2 iridium sites through polysilicon lines to the probe back end and then across 4-μm-thick parylene-encased electroplated-gold folding lead transfers to the associated platform. Three levels of interconnect with a 10-μm minimum pitch are utilized for the 32 leads that traverse the platforms. After rapid microassembly, micromachined latches are used to fasten the folded device. Two flexible parylene cables with gold leads at a 20-μm pitch are monolithically integrated with the probes to minimize tethering and avoid any need for lead bonding within the array, and these cables carry the neural signals to a remote circuit module or percutaneous connector. With thin ($\sim$15-μm) boron-doped shanks at a $\sim$200-μm pitch, the array displaces only 1.7% of the 0.64-mm^2 instrumented tissue area, assuming a 100-μm recording range. Neural signals were recorded *in vivo* from the guinea pig auditory cortex. [2010-0200]**

***Index Terms*—Cortical prosthesis, microelectrode array, neural mapping, neuroprosthetics, silicon probe, three-dimensional assembly of microelectromechanical devices.**

I. Introduction

NEUROPROSTHETIC devices are developed to replace lost sensory functions, e.g., hearing [1]–[3] and sight [4], [5], and to control paralyzed and prosthetic limbs [5]–[7]. The fundamental element of these devices is the electrode array that interfaces with the neural tissue. Arrays are also used in basic neuroscience research to investigate the neuronal circuits within the central nervous system. The conceptual design of the cortical electrode system shown in Fig. 1 includes a penetrating electrode array and implantable signal processing and telemetry circuitry. For most applications, the array should have a significant number of stimulation and/or recording sites arranged in three-dimensions, a very small implanted volume to minimize invasiveness, and a small platform area and low vertical rise above the cortical surface to allow the replacement of the *dura mater* and prevent the tethering of the implant to the skull [7], [8]. For passive high-density interfaces, creative design and processing techniques are essential to assuage the inherent interconnect and bonding difficulties associated with large numbers of sites.

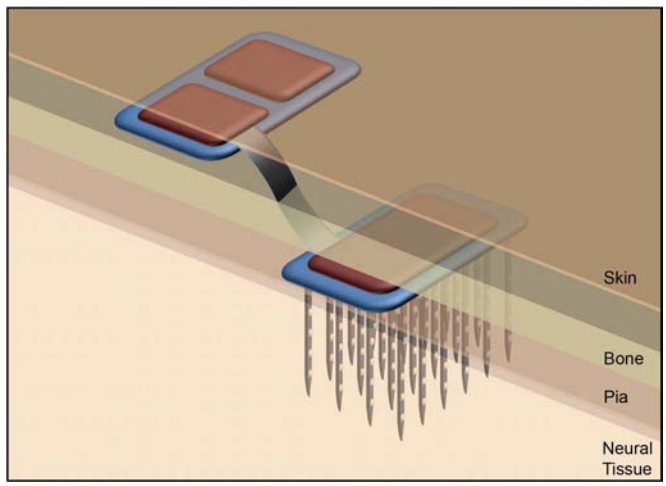

Fig. 1. Conceptual arrangement of an implantable cortical microsystem.

Revolutionary advances in neuroscience are enabled by planar 2-D electrode arrays fabricated using silicon micromachining technology [9]. Both boron etch-stop and silicon-on-insulator (SOI) processes can provide high yield and the selectivity necessary to release very thin structures, thus meeting the prerequisite of minimal tissue displacement [9]. Although 3-D arrays microassembled using planar probes with thin (5–15-μm) shanks have been reported, their availability to the neuroscience community and their practicality for neuroprosthetic systems has been limited, in part due to large platform sizes and/or difficult assembly operations. Some of these devices have used 2-D probes threaded through slots in a thin platform and secured with spacers [10]–[13]. Other authors have stacked probes using hybrid cables [14], although the size of the mounting structure/platform was not reported. To develop a truly low-rise ($\sim$500-μm) platform using a robust assembly process, another design [15] exchanged the thin platform for a thicker platform with slots to precisely align the probes and used a polymer overlay bonded to the platform to cable

Manuscript received June 30, 2010; revised January 11, 2011; accepted January 22, 2011. Date of publication April 11, 2011; date of current version June 2, 2011. This work was supported in part by the Engineering Research Centers Program, in part by the National Science Foundation (NSF) under Grant ERC-9986866, and in part by a gift from Ms. Polly Anderson. Subject Editor A. J. Ricco.

Sister M. E. Merriam was with the Department of Electrical Engineering and Computer Science, University of Michigan, Ann Arbor, MI 48105 USA. She is now with St. Dominic Savio Catholic High School, Austin, TX 78717 USA (e-mail: sisterme@umich.edu).

O. Srivannavit is with the Department of Chemical Engineering, University of Michigan, Ann Arbor, MI 48105 USA (e-mail: onnops@umich.edu).

M. N. Gulari and K. D. Wise are with the Engineering Research Center for Wireless Integrated Microsystems, Department of Electrical Engineering and Computer Science, University of Michigan, Ann Arbor, MI 48105 USA (e-mail: toning@eecs.umich.edu; wise@umich.edu).

Color versions of one or more of the figures in this paper are available online at http://ieeexplore.ieee.org.

Digital Object Identifier 10.1109/JMEMS.2011.2127450

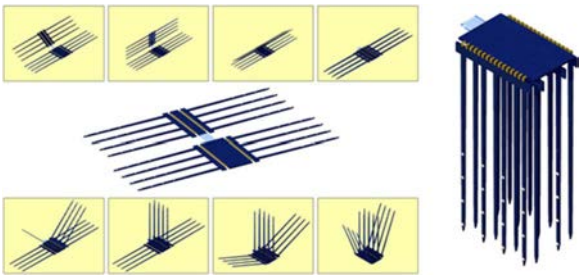

Fig. 2. Conceptual formation of the folding assembly. This example layout combines what would traditionally be thought of as four 2-D probes and the portion of the mounting platforms that would span the space between them.

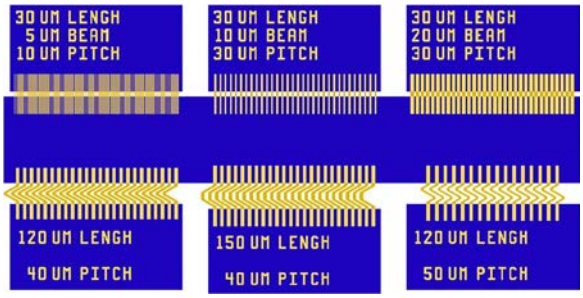

Fig. 3. Layout of six selected beam-bending test structures. More than 30 variations were fabricated.

the leads to adjacent circuitry or to a percutaneous connector. Two-probe folding structures with low site counts ($\leq$ 12 sites in total) have also been reported [16]–[18], but although larger site counts are more practical for neuroscience and neuroprosthetic needs, they also significantly increase the assembly and lead transfer challenges. This paper describes a folding probe design that meets the 3-D minimum-volume small-platform low-rise requirements while also integrating cables with the probes to eliminate all platform-associated bonding [19], [20]. The resulting four-probe 64-site device can rapidly be formed from a single microfabricated structure.

II. Array Design and Fabrication

A. Conceptual Overview

A folding scheme applied to electrode arrays can directly integrate individual probes, electrical interconnects, and their corresponding platforms at the device layout level. This architecture decreases the lateral platform span and vertical rise. Reduced assembly time and increased yield were also target objectives of the technique.

A conceptual layout and assembly process is illustrated in Fig. 2. When four probes are incorporated into one array, the leads from the smaller bottom platform can travel across the foldable platform connector cable to the wider top platform, and then, all of the leads can come off the array on a single cable. Alternatively, individual flexible cables can leave the array from both the top and bottom platforms. The assembly consists of folding the structure in half to place the smaller bottom platform vertically on top of the larger top platform, bending the probes orthogonal to the platforms and then securing the device. The lateral dimension of the platform is not significantly larger than the area of tissue instrumented, and no platform overhang is necessary. The overall vertical rise is a combination of the heights due to the probe back end, foldable interconnects, and platform thickness. With the platforms fabricated as part of the same process as the probes, this height can be a few hundred micrometers or less.

The number of electrode sites and shanks, as well as their dimensions and spacings, can be varied as the application requires, although the minimum platform width becomes constrained by the pitch and number of lead lines, unless multiple levels of interconnect are employed. Multiplexing circuitry located on the array would help decrease the number of external leads and ease the constraints on platform width and probe spacing. If an active fabrication process is used, circuits can directly be incorporated on the probe back end or the platform; similarly, hybrid chips could be used.

B. Bending Test Structures

Because the strength of the folded structure, the continuity of the interconnects, the radius of curvature of the bends, and the structural stabilization mechanisms are all essential aspects of the design, test structures and proof-of-concept devices were made. The main parameters that influence interconnect folding are the material and shape of the bendable leads, as well as their length, width, pitch, and number. The beam-bending test structures shown in Fig. 3 consisted of a main silicon platform that corresponds to the array platform, with a number of silicon tabs representing back ends of probes. The beams that connect the platform and tabs were electroplated gold, and they were not encapsulated, providing an opportunity to focus on the interconnect parameters, independent of the insulation.

The designs included straight and zigzag-shaped beams. The angled beams were devised to improve the top-side anisotropic etching of the underlying silicon [stopped by the self-limiting V-groove formed by the (111) planes] by increasing the effective etch opening [13]. Straight beams were also tested. Because the wet etch continued until the integrated cables were fully released, the straight beams were both functional and of a simpler design.

All of the variations of the beam-bending test structures were fully released; therefore, bending was possible. It was significantly easier to place the fold along the silicon platform edge than to fold the beams precisely at the center, as originally intended in some designs. Repeated bending tests (from approximately 0° to approximately 90°) were used to assess the design strength. Most designs (fabricated with 4-μm-thick electroplated-gold beams) withstood more than 20 such bends. Because the beams need to withstand only a single bend during the assembly process, this approach was judged more than adequate. Wider and longer beams withstood more bending, as did the zigzag designs. However, although the longer beams tended to curve as the tab was brought to the 90° position, the shorter beams had a sharper better defined bend location. Advanced jigs would improve bend placement.

The thickness of the foldable interconnects affects durability and final device positioning. Three thicknesses (2, 4, and 6 μm) of electroplated gold over a 50-nm-thick chromium adhesion layer, all without encapsulation, were evaluated. The folding leads were fabricated by depositing 50 nm of chromium

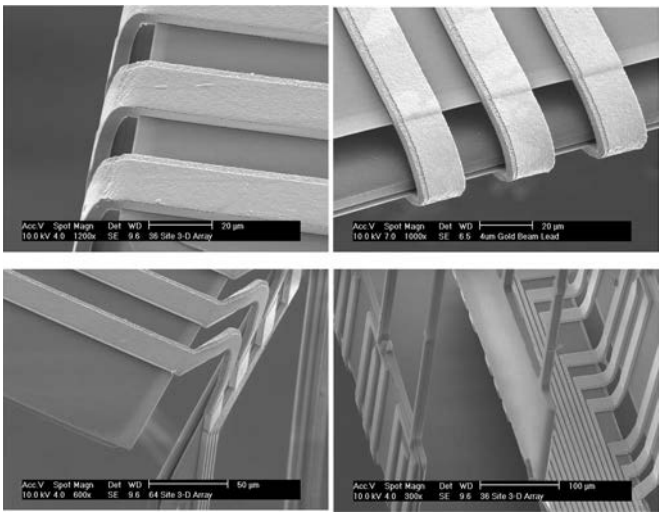

Fig. 4. Scanning electron microscopy (SEM) images of the folded bending test structures.

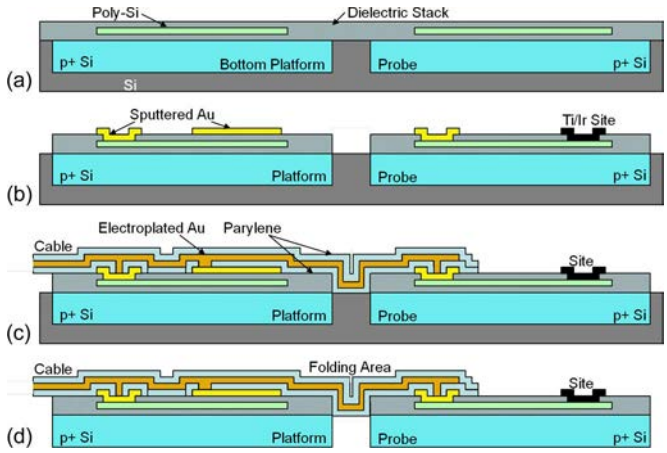

Fig. 5. Process flow for the folded arrays.

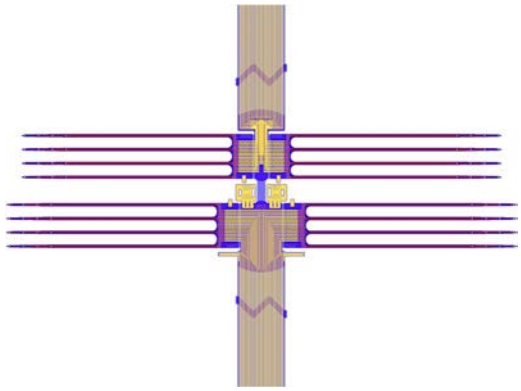

Fig. 6. Layout of the 64-site array.

covered by 200 nm of gold, opening the folding lead areas in photoresist, gold plating the leads to the desired thicknesses, stripping the resist, and etching away the exposed Cr–Au seed layer. The 2-μm-thick leads easily tore, and the 6-μm leads were excessively stiff, giving rise to adhesion and bending problems. Fig. 4 shows fabricated test devices with 4-μm-thick beams, including one beam that was once overbent. Although, at the fold, the outer surface appears to have small cracks due to stretching, the interconnect path is not compromised. The 4-μm thickness was selected as optimal due to its ease of bending and resilience during repeated bending and during overbending.

C. Two-Dimensional Layout and Fabrication

Previous work at the University of Michigan formed the basis for the process flow for this 3-D 64-site folded electrode array [13], [21]–[23], as shown in Fig. 5. Fabrication begins with a selective boron diffusion, forming a 12-μm-deep etch stop to define the substrate for the penetrating shanks and back-end bonding area. A stress-compensated dielectric stack (300-nm SiO_2/150-nm Si_3N_4/300-nm SiO_2) is then deposited, and a 600-nm-thick polysilicon layer is deposited and patterned for interconnects on the shanks, back ends, and bottom platform. Another dielectric stack (300-nm SiO_2/150-nm Si_3N_4) is used to encapsulate the polysilicon [see Fig. 5(a)]. Contacts are opened, titanium and iridium (50 and 150 nm, respectively) are sputtered onto the shanks to form the sites, and chromium and gold (50 and 300 nm, respectively) are deposited for the second-layer interconnects on the bottom platform**.** The field dielectric layers are then removed using reactive ion etching to expose the silicon underneath [see Fig. 5(b)]. A 2-μm-thick parylene film is next deposited, and contacts are opened through it using an O_2 plasma. Gold leads (4 μm thick) are next defined and electroplated on the parylene cables and for top-layer interconnects on the top and bottom platforms. A second 3-μm-thick parylene film is then deposited and patterned to encapsulate the electroplated gold and define the shape of the folding areas, the latches, and the cables [see Fig. 5(c)]. The wafer is thinned from the back side using the deep reactive ion etching and is then etched in tetramethyl ammonium hydroxide (TMAH) with ammonium persulfate at 80 °C until the probes are released from the wafer [see Fig. 5(d)].

A 64-site array was developed using this process, consisting of four four-shank probes with four electrode sites per 3-mm-long shank and two integrated cables, one from each platform. The 177-μm^2 iridium sites were on 200-μm centers along each shank, and the shanks were on a 200-μm pitch. The array layout is shown in Fig. 6. Interconnect lines travel from the sites to the probe back end and across folded lead transfers to their associated platform. Two flexible parylene cables are monolithically integrated to minimize tethering and eliminate bonding within the array. The folded lead transfers are formed from 4-μm-thick 17-μm-wide electroplated-gold beams, insulated with parylene in the same process used to form the cables. To keep the shank width narrow, the typical 9-μm polysilicon pitch on the shank tapers to 2-μm leads with 2-μm spaces around the electrode sites. The main shank width of 46 μm decreases to 31 μm as leads reach their designated sites. With a total shank thickness of approximately 14.75 μm (including the dielectrics, interconnects, and sites) the shank cross-sectional area at the uppermost site is 678.5 μm^2. Based on an electrical recording range of 100 μm [24], [25], the instrumented tissue cross-sectional area is 0.64 mm^2. The array occupies only 1.7% of this instrumented area.

TABLE I
FOLD ARRAY STRUCTURE SPECIFICATIONS

		Top	*Bottom*
Back-ends	Width	600 μm	200 μm
	Length	1033 μm	1033 μm
Platform	Height	320 μm	300 μm
	Width	646 μm	646 μm

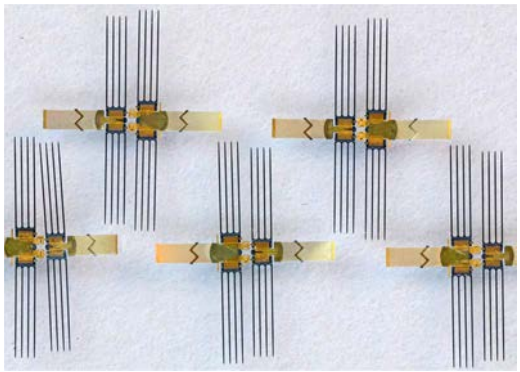

Fig. 7. Photograph of five devices prior to assembly.

On the probe back ends, leads are transferred from polysilicon to electroplated-gold interconnects. The 320-μm-high back ends incorporate triple polysilicon-gold-integrated contacts per lead. This height of the probe back end can be reduced to less than half using single contacts. Parylene-encapsulated foldable lead transfers that connect the back ends and the platforms are formed using 17-μm-wide gold beams on a 29-μm pitch. For the top platform, electroplated gold encapsulated with parylene (with a 10-μm width and a 17-μm pitch) was used for leads for design simplicity and lower resistance. For the bottom platform, multilevel interconnect is required, because its width is only 1/3 of the top platform. The process flow incorporates a polysilicon layer, the electroplated-gold layer, and a sputtered gold layer as interconnects (a 6-μm lead width and a 10-μm pitch) on the bottom platform. These leads transfer to the cable-level electroplated-gold interconnects at the mushroom-shaped cable base. The dimensions of the probe back ends and the platforms are presented in Table I.

As aforementioned, one of the advantages of this design is that no connections between the probes and the platform need to be bonded after release. Once assembled, the cables are aligned directly on top of each other, thus forming a version of multilevel interconnect. The cables use a 20-μm lead pitch, are less than 750 μm wide, and are 2 mm long. Short cables were included in this version, but their length can be increased as a given application requires. Figs. 7 and 8 show the fabricated devices.

D. Latches

Two latch structures, the cable clasp and the platform gate, as shown in Fig. 9, were developed to maintain the folded probe position until the assembly has been secured with a sealant. The cable clasp consists of a foldable interconnect in an encapsulating sheath and protrudes from the top cable near the platform region. After the bottom platform is vertically placed on top of the top platform, the cable clasps on each side are

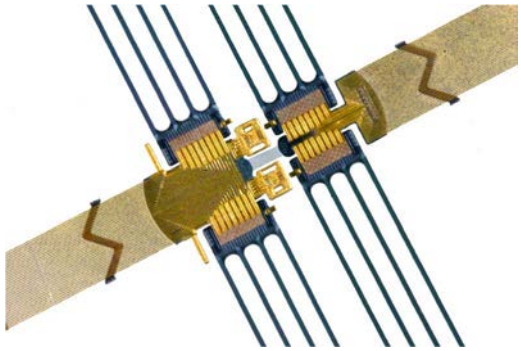

Fig. 8. Close-up photograph of a device prior to assembly, with the background removed from the photograph. The integrated cables are shown leaving the mushroom-shaped part of the platforms. For this structure, alternating foldable interconnects were electroplated gold, and the remaining lead transfers and the cable lines were sputtered gold.

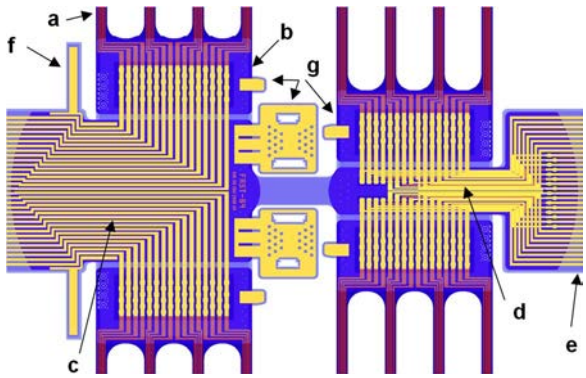

Fig. 9. Layout of the central portion of the device showing (a) the shanks transitioning to the (b) back end, (c) the top platform, and (d) the bottom platform, (e) the cable, and (f) the cable clasp and (g) platform-gate latch structures.

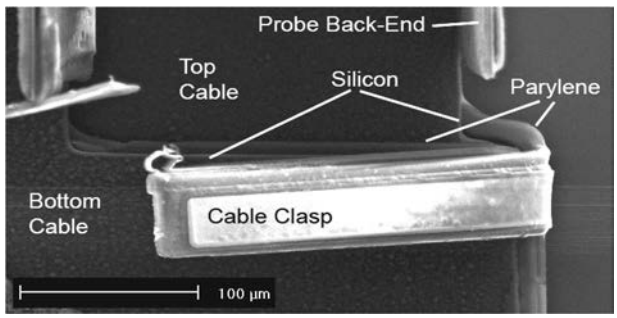

Fig. 10. SEM of the folded cable clasp latching the top and bottom cables.

bent around the bottom cable, as shown in Fig. 10, keeping the two cables aligned and the two platforms in contact. Assembly experience has verified the utility of this structure, particularly during the remaining folding steps, and wider or additional clasps would further improve the design.

The platform gates consist of silicon fins on the probe back ends and foldable gates that are attached to the top platform. Once the probes have been in position, the gates are bent upward, latching the fins to limit the range of motion of the probes, as shown in Fig. 11. The design of both parts was carefully considered to ensure smooth interlocking during the assembly. Trials with this structure demonstrated its merit, particularly for the top platform probes. Although it also works for the

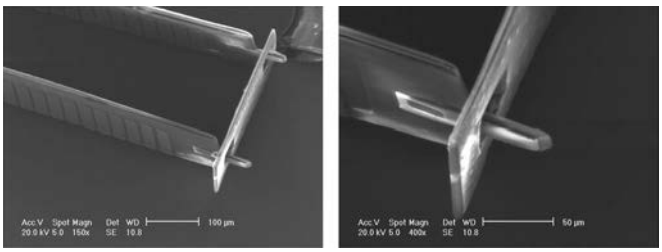

Fig. 11. SEM images of the platform-gate latch test structure showing the silicon fins in the latch hole with the gate fully in place (left) and with partial gate closure (right) due to the lack of sufficient prebending.

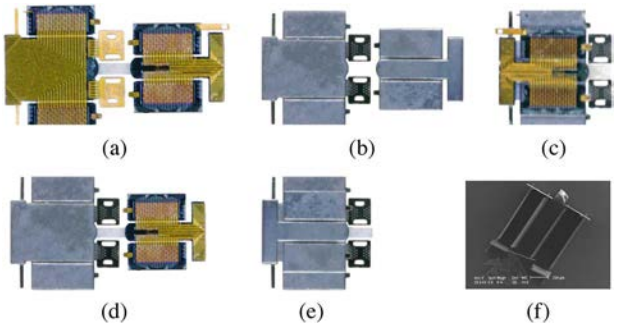

Fig. 12. Simplified assembly steps illustrated with latch test structures that were designed without probe shanks. (a) Top view of the structure showing bendable gold interconnects and parylene intermediary cable. (b) Bottom view. (c) First fold in the assembly process. (d) After the rotation of smaller bottom platform. (e) Second fold and platform alignment. (f) Remaining folds of the probes and the cable clamps and platform-gate latches.

bottom platform probes, more careful assembly is necessary to ensure proper engagement. Further iteration to tighten the tolerances would enhance the design, as would the development of a similar latch for the other back-end edge.

III. Three-Dimensional Assembly

The general assembly procedure is illustrated in Fig. 12. The stage consisted of a metal support base, foam cushion, and latex cover. Assembly occurred "upside down," with shanks pointing upward after the bending has been complete; thus, what was actually the top platform was on the bottom of the assembly stack. The device was held with a glass cover slip over the larger top platform and its cable. Then, the platform latches and probes were prebent more than 90° and unbent, and this approach eased the later bending.

In the final position, the two platforms were aligned on top of each other, both face down. This direction was chosen so that the platform edges delineate the bend locations and also because it reduces the risk of the parylene peeling off of the silicon. The assembly tool was used to manually fold the smaller bottom platform and its cable over the top platform. At this stage, the top platform was face down but the bottom platform was face up. To form the necessary twist in the platform connector cable, the bottom platform was then guided in a semicircle around to its original position, still face up. Again, the bottom platform was folded on top of the top platform, and both platforms were then face down. Because the individual platforms were thin, this stacking did not significantly increase the total height. At this stage, the two platforms were aligned, and the cable clamps were folded over.

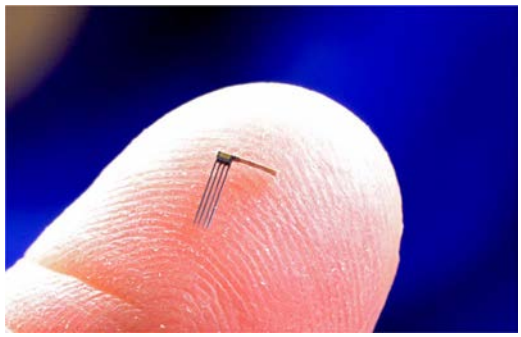

Fig. 13. Folded 64-site 3-D microelectrode array on a fingertip.

The four probes were individually bent upward. The manual-bending techniques used here could position the different probes parallel to within a few degrees of normal; however, using a deep reactive-ion etching (DRIE)-formed bonding jig, it should be possible to control the angles to well within 1° of normal (to better than 20 μm over a 2-mm shank length) and to lock this in through the potting process. The back ends connected to the bottom platform were designed to be shorter than the back ends attached to the top platform to compensate for the platform thickness. After fine-tuning the probe angles, the platform-gate latches were moved into position. Medical-grade silicone was placed in the trenches formed by the platforms and probe back ends to finalize the angle and further encapsulate the device, and surface tension assisted in drawing the adhesive into the trenches. Epoxy (353ND and 353ND-T, Epoxy Technology, Inc.) can be used instead for chronic implantation. The assembly takes less than 25 min, and a folded device photograph is presented in Fig. 13.

IV. *In Vivo* Results

Folded arrays were acutely implanted through the *pia* into the auditory cortex of a guinea pig to explore insertion and recording performance *in vivo*. The typical surgical preparation of the recording experiments was detailed as follows. Pigmented guinea pigs (Elmhill Farms) were used in these studies. The animals were deeply anesthetized throughout the entire procedure using ketamine (40 mg/kg) and xylazine (10 mg/kg), and at no time were the animals allowed to awaken. Stainless steel screws were inserted into the skull to anchor the subject to a rigid bar for stabilization during surgery and recording, which took place in a double-walled sound booth. After a craniotomy in the skull overlying the auditory cortex, the dura was cut. The array was implanted using a vacuum pick mounted to a micromanipulator for direct visual placement in the auditory cortex. The animal ground was defined by connecting the neck muscles to the ground and reference pins of the headstage. The acoustic stimulus was provided through a Beyer speaker. These procedures were in accordance with the National Institutes of Health (NIH) *Guidelines for the Use and Care of Laboratory Animals* (NIH Publication 80–23) and the guidelines of the University of Michigan Committee on the Use and Care of Animals. Insertion through the pia was easily accomplished

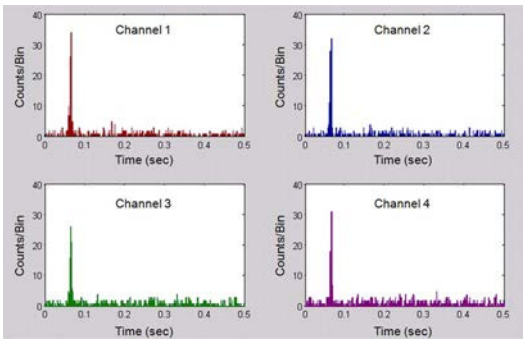

Fig. 14. PSTHs of spike count for four channels of the 3-D array based on *in vivo* recordings of elicited responses to acoustic noise bursts (onset time = 0.05 s) in the auditory cortex of a guinea pig.

with minimal dimpling of the cortical surface, similar to our experience with microassembled arrays of comparable size. The 177-μm^2 Ir sites had 1-kHz impedance levels between 0.5 and 1.0 MΩ, consistent with other reported sites of this size [1]. Connections to the recording system headstage were made through a printed circuit board (PCB) probe stalk to which the array cables were mounted and bonded. Acoustic noise bursts were used to obtain elicited responses. Fig. 14 shows the acquired peristimulus time histograms (PSTHs) of spike count versus time bin for the four channels. The PSTH is one of the main visualization tools for the verification of neural responses. The recorded histograms exhibit the expected response patterns for this acoustic stimulus and recording location.

V. Conclusion

By employing a folding topology, the design that has been presented uses only one additional mask to enable a folded 3-D structure following a standard chronic 2-D probe process. The minimum-volume small-platform low-rise nature of the architecture makes it suitable for cortical applications. The four-probe structure with sites arranged at a 200-μm pitch in all three directions tailors the device to 3-D neuroscience studies. The fabrication process is compatible with the formation of signal processing electronics to amplify signal levels and minimize output lead counts by multiplexing. With the addition of integrated or hybrid circuits, the 3-D system could include implantable signal processing and telemetry for bidirectional (stimulate/record) neuroprosthetic applications.

Acknowledgment

The authors would like to thank B. Casey for the bonding and packaging, Sr. M. R. Villareal for the impedance testing, and J. Wiler for the *in vivo* testing.

References

[1] M. E. Merriam, S. Dehmel, O. Srivannavit, S. E. Shore, and K. D. Wise, "A three-dimensional 160-site microelectrode array for cochlear nucleus mapping," *IEEE Trans. Biomed. Eng.*, vol. 58, no. 2, pp. 397–403, Feb. 2011.

[2] A. C. Johnson and K. D. Wise, "A robust batch-fabricated high-density cochlear electrode array," in *Proc. IEEE 23rd Int. Conf. MEMS*, Hong Kong, Jan. 2010, pp. 1007–1010.

[3] D. J. Anderson, "Penetrating multichannel stimulation and recording electrodes in auditory prosthesis research," *Hear. Res.*, vol. 242, no. 1/2, pp. 31–41, Aug. 2008.

[4] E. Margalit, M. Maia, J. D. Weiland, R. J. Greenberg, G. Y. Fujii, G. Torres, D. V. Piyathaisere, T. M. O'Hearn, W. Liu, G. Lazzi, G. Dagnelie, D. A. Scribner, E. de Juan, Jr., and M. S. Humayun, "Retinal prosthesis for the blind," *Surv. Ophthalmol.*, vol. 47, no. 4, pp. 335–356, Jul./Aug. 2002.

[5] R. A. Normann, "Technology insight: Future neuroprosthetic therapies for disorders of the nervous system," *Nat. Clin. Pract. Neurol.*, vol. 3, no. 8, pp. 444–452, Aug. 2007.

[6] A. B. Schwartz, "Cortical neural prosthetics," *Annu. Rev. Neurosci.*, vol. 27, pp. 487–507, Jul. 2004.

[7] M. A. Lebedev and M. A. L. Nicolelis, "Brain–Machine interfaces: Past, present and future," *Trends Neurosci.*, vol. 29, no. 9, pp. 536–546, Sep. 2006.

[8] K. D. Wise, A. M. Sodagar, Y. Yao, M. N. Gulari, G. E. Perlin, and K. Najafi, "Microelectrodes, microelectronics, and implantable neural microsystems," *Proc. IEEE*, vol. 96, no. 7, pp. 1184–1202, Jul. 2008.

[9] K. D. Wise, "Silicon microsystems for neuroscience and neural prostheses," *IEEE Eng. Med. Biol. Mag.*, vol. 24, no. 5, pp. 22–29, Sep./Oct. 2005.

[10] A. C. Hoogerwerf and K. D. Wise, "A three-dimensional microelectrode array for chronic neural recording," *IEEE Trans. Biomed. Eng.*, vol. 41, no. 12, pp. 1136–1146, Dec. 1994.

[11] Q. Bai, K. D. Wise, and D. J. Anderson, "A high-yield microassembly structure for three-dimensional microelectrode arrays," *IEEE Trans. Biomed. Eng.*, vol. 47, no. 3, pp. 281–289, Mar. 2000.

[12] M. D. Gingerich, J. F. Hetke, D. J. Anderson, and K. D. Wise, "A 256-site 3-D CMOS microelectrode array for multipoint stimulation and recording in the central nervous system," in *Proc. Int. Conf. Solid-State Sensors Actuators (Transducers)*, Munich, Germany, Jun. 2001, pp. 416–419.

[13] Y. Yao, M. N. Gulari, J. A. Wiler, and K. D. Wise, "A microassembled low-profile three-dimensional microelectrode array for neural prosthesis applications," *J. Microelectromech. Syst.*, vol. 16, no. 4, pp. 977–988, Aug. 2007.

[14] N. B. Langhals and D. R. Kipke, "Validation of a novel three-dimensional electrode array within auditory cortex," in *Proc. 31st Annu. Int. IEEE Conf. EMBS*, Minneapolis, MN, 2009, pp. 2066–2069.

[15] G. E. Perlin and K. D. Wise, "A compact architecture for three-dimensional neural microelectrode arrays," in *Proc. 30th Annu. Int. IEEE Conf. EMBS*, Vancouver, Canada, Sep. 2008, pp. 5806–5809.

[16] P. J. Rousche, D. S. Pellinen, D. P. Pivin, Jr., J. C. Williams, R. J. Vetter, and D. R. Kirpe, "Flexible polyimide-based intracortical electrode arrays with bioactive capability," *IEEE Trans. Biomed. Eng.*, vol. 48, no. 3, pp. 361–371, Mar. 2001.

[17] S. Takeuchi, T. Suzuki, K. Mabuchi, and H. Fujita, "3-D flexible multichannel neural probe array," *J. Micromech. Microeng.*, vol. 14, no. 1, pp. 104–107, Jan. 2004.

[18] S. C. Chuang, C. H. Chen, H. C. Su, S. R. Yeh, and D. J. Yao, "Design and fabrication of flexible neural microprobe for three dimensional assembly," in *Proc. IEEE Int. Conf. MEMS*, Hong Kong, Jan. 2010, pp. 1003–1006.

[19] M. E. Merriam, "A three-dimensional bidirectional interface for neural mapping studies," Ph.D. dissertation, Dept. Elect. Eng., Univ. Michigan, Ann Arbor, MI, 2010.

[20] M. E. Merriam, O. Srivannavit, and K. D. Wise, "A 64-site three-dimensional folded electrode array using planar fabrication," in *Proc. Annu. Fall Meeting Biomed. Eng. Soc.*, Austin, TX, Oct. 2010.

[21] K. Najafi, K. D. Wise, and T. Mochizuki, "A high-yield IC-compatible multichannel recording array," *IEEE Trans. Electron Devices*, vol. ED-32, no. 7, pp. 1206–1211, Jul. 1985.

[22] Y. Yao, M. N. Gulari, B. Casey, J. A. Wiler, and K. D. Wise, "Silicon microelectrodes with flexible integrated cables for neural implant applications," in *Proc. 3rd Int. IEEE EMBS Conf. Neural Eng.*, Kohala Coast, HI, 2007, pp. 398–401.

[23] G. E. Perlin and K. D. Wise, "Ultracompact integration for fully implantable neural microsystems," in *Proc. IEEE 22nd Int. Conf. MEMS*, Sorrento, Italy, 2009, pp. 228–231.

[24] D. A. Henze, Z. Borhegyi, J. Csicsvari, A. Mamiya, K. D. Harris, and G. Buzsáki, "Intracellular features predicted by extracellular recordings in the hippocampus *in vivo*," *J. Neurophysiol.*, vol. 84, no. 1, pp. 390–400, Jul. 2000.

[25] V. S. Polikov, P. A. Tresco, and W. M. Reichert, "Response of brain tissue to chronically implanted neural electrodes," *J. Neurosci. Methods*, vol. 148, no. 1, pp. 1–18, Oct. 2005.

Sister Mary Elizabeth Merriam received the B.S. degree from Rensselaer Polytechnic Institute, Troy, NY, in 1999, and the M.S. and Ph.D. degrees from the University of Michigan, Ann Arbor, in 2001 and 2010, respectively, all in electrical engineering.

During her undergraduate years, she was an Intern at Eastman Kodak Company. In 2002, she entered the Dominican Sisters of Mary, Mother of the Eucharist. From 2000 to 2002 and 2007 to 2010, she was a Research Assistant at the Center for Wireless Integrated MicroSystems. She is currently the Science Department Chair and a Teacher at St. Dominic Savio Catholic High School, Austin, TX. Her research interests include electrode arrays for neural interfaces.

Onnop Srivannavit received the B.S. degree in chemical technology and the M.S. degree in petrochemical technology from Chulalongkorn University, Bangkok, Thailand, and the Ph.D. degree in chemical engineering from the University of Michigan, Ann Arbor, in 2002.

He is currently a Research Engineer in the Department of Chemical Engineering, University of Michigan. His research interests include the development of MEMS and microfluidic devices for biomedical and environmental applications.

Mayurachat Ning Gulari received the B.S. degree in chemical technology and the M.S. degree in polymer science and engineering from the Petroleum and Petrochemical College, Chulalongkorn University, Bangkok, Thailand, in 1993 and 1995 respectively.

She was a Planning Engineer with Star Petroleum Refining Company, Rayong, Thailand, where she worked on the optimization and planning of feedstock purchases and the refinery products mix. In 1996, she became a Research Engineer in the Display Technology Center, University of Michigan, Ann Arbor, where for the last ten years, she has been a Senior Research Engineer in the Engineering Research Center for Wireless Integrated Microsystems. Her research interests include designing and fabricating implantable micromachined probes for drug delivery, neural signal recording, and stimulation.

Kensall D. Wise (S'61–M'69–SM'83–F'86–LF'06) received the B.S.E.E. (with the highest distinction) degree from Purdue University, West Lafayette, IN, in 1963, and the M.S. and Ph.D. degrees in electrical engineering from Stanford University, Stanford, CA, in 1964 and 1969, respectively.

From 1963 to 1965 and from 1972 to 1974, he was a member of Technical Staff at Bell Telephone Laboratories, Murray Hill, NJ, where his work focused on the exploratory development of integrated electronics for use in telephone communications. From 1965 to 1972, he was a Research Assistant and then a Research Associate and Lecturer in the Department of Electrical Engineering, Stanford University, working on the development of micromachined solid-state sensors. In 1974, he joined the Department of Electrical Engineering and Computer Science, University of Michigan, Ann Arbor, where he is currently the J. Reid and Polly Anderson Professor of Manufacturing Technology, the Director of the Engineering Research Center for Wireless Integrated Microsystems, and the Director of the Lurie Nanofabrication Facility. His current research is focused on the development of integrated microsystems for health care, environmental monitoring, and defense applications.

Dr. Wise is a Fellow of the American Institute for Medical Biological Engineering (AIMBE) and is a member of the U.S. National Academy of Engineering. He organized and served as the first Chairman of the Technical Subcommittee on Solid-State Sensors of the IEEE Electron Devices Society (EDS). He was the General Chairman of the 1984 IEEE Solid-State Sensor Conference, served as the IEEE EDS National Lecturer in 1986 and was the Technical Program Chairman in 1985 and the General Chairman in 1997 of the IEEE International Conference on Solid-State Sensors, Actuators, and Microsystems. He is the recipient of the Paul Rappaport Award from the EDS in 1990, the Distinguished Faculty Achievement Award from the University of Michigan in 1995, the Columbus Prize from the Christopher Columbus Fellowship Foundation in 1996, the 1997 SRC Aristotle Award, and the 1999 IEEE Solid-State Circuits Field Award. In 2002, he was named the William Gould Dow Distinguished University Professor by the University of Michigan and held the 2007 Henry Russel Lectureship with the University.